

Research Article

Duaa Al-Jeznawi, Ismacahyadi Bagus Mohamed Jais*, Bushra S. Albusoda, and Norazlan Khalid

Numerical modeling of single closed and open-ended pipe pile embedded in dry soil layers under coupled static and dynamic loadings

<https://doi.org/10.1515/jmbm-2022-0055>

received March 26, 2022; accepted May 13, 2022

Abstract: For the design of a deep foundation, piles are presumed to transfer the axial and lateral loads into the ground. However, the effects of the combined loads are generally ignored in engineering practice since there are uncertainties to the precise definition of soil–pile interactions. Hence, for technical discussions of the soil–pile interactions due to dynamic loads, a three-dimensional finite element model was developed to evaluate the soil pile performance based on the 1 g shaking table test. The static loads consisted of 50% of the allowable vertical pile capacity and 50% of the allowable lateral pile capacity. The dynamic loads were taken from the recorded data of the Kobe earthquake. The current numerical model takes into account the material non-linearity and the non-linearity of pile-to-surrounded soil contact surfaces. A lateral ground acceleration was adapted to simulate the seismic effects. This research emphasizes modeling the 1 g model by adapting MIDAS GTS NX software. This will, in turn, present the main findings from a single pile model under a combined static and dynamic load. Consequently, the main results were first validated and then used for further deep investigations. The numerical results predicted a slightly

higher displacement in the horizontal and vertical directions than the 1 g shaking table. The shear stress–shear strain relationship was predicted. Positive frictional resistance for the closed-ended pile was captured during the first 5 s when low values of acceleration were applied and, consequently, the pile resistance decreased and became negative. Internal and external frictional resistance was captured for the open-ended pipe pile. Overall, frictional resistance values were decreased with time until they reached the last time step with a minimum value. As a result, the evaluation of the current study can be used as a guide for analysis and preliminary design in engineering practice.

Keywords: numerical modeling, coupled static–dynamic load, plug soil, frictional resistance, shear stress reversal

1 Introduction

The impact of dynamic soil–structure interaction on structural seismic response has lately increased the interest of researchers and engineers all around the world. In many situations, in addition to vertical loads, piles transfer lateral forces caused by strong winds, earthquakes, slope failures, and liquefaction-induced lateral spread. As a result, a pile can be subjected to the combined action of vertical and horizontal loads, depending on the nature of the construction. Hence, research into pile behavior under lateral and combined loads is crucial. The behavior of a single pile in sandy soils was studied under the effect of the combination of vertical and lateral loadings by Achmus and Thieken [1]. The results showed that the interaction effect is attributed to this combination of loadings because of the passive ground pressure and the pile skin friction mobilized at the same time due to the lateral and vertical loads, respectively.

Several studies have been done to investigate the non-constraint of ground attitudes. Kokusho and Iwatate [2] developed a flexible sandy soil box to perform a lab

* **Corresponding author: Ismacahyadi Bagus Mohamed Jais**, School of Civil Engineering, College of Engineering, Universiti Teknologi MARA Shah Alam, 40450, Selangor, Malaysia, e-mail: ismac821@uitm.edu.my

Duaa Al-Jeznawi: School of Civil Engineering, College of Engineering, Universiti Teknologi MARA Shah Alam, 40450, Selangor, Malaysia; Lecturer at College of Engineering, Al-Nahrain University, Baghdad, Iraq, e-mail: 2021286852@student.uitm.edu.my

Bushra S. Albusoda: School of Civil Engineering, College of Engineering, University of Baghdad, Baghdad, Iraq, e-mail: dr.bushra_albusoda@coeng.uobaghdad.edu.iq

Norazlan Khalid: School of Civil Engineering, College of Engineering, Universiti Teknologi MARA Shah Alam, 40450, Selangor, Malaysia, e-mail: norazlan0481@salam.uitm.edu.my

experiment. The main considerations for a flexible box are maintaining a uniform section during the application of the seismic load, allowing the soil to move freely with no resistance and keeping minimum shear strength. Therefore, the “free field” motion is referred to the soil response of a specific location without any structural constraints. Since soil layers have different strengths, the lateral movement of layers due to earthquakes may significantly differ. The effect of the soil non-linear models has been studied by Kim and Roesset [3]. The results showed that the parameters of the constitutive model have a significant role in simulating dynamic soil–structure interaction. Numerical analyses can control some of the drawbacks of experimental models, such as scaling [4,5], allowing for the validation of experimental findings, and a deeper understanding of various soil–pile interaction features. Different studies used laboratory experiments [6] and the three-dimensional (3D) finite element method to assess the behavior of piles under lateral loads [7].

This study was developed to investigate the influence of a simultaneous load combination of static loads (vertical and lateral loads) combined with dynamic loads (earthquake) on closed and open-ended pipe piles embedded in sandy soil layers. A 3D numerical model has been developed using MIDAS GTS NX software. The main simulation findings of the closed-ended pipe pile are validated with the 1 g shaking table tests performed in the laboratory by Hussein and Albusoda [8]. As for the open-ended pipe pile, the length of the soil plug was modeled as $4D_{\text{inner}}$ ¹ the entrance of soil will continue until the inner soil cylinder mode develops sufficient resistance to prevent further soil intrusion. If the stresses in the inner soil are sufficient to prevent further soil intrusion inside the pipe pile, the pile will act as a fully plugged (closed-ended) pile. The results of the current models are valuable to evaluate post-earthquake behavior. The main objective of this study is to assess the influence of earthquakes on the dynamic response of a single pile loaded with vertical and static lateral loads, whereby the pile is embedded in layers of dry sand with different densities.

2 Research methodology

This study aims to identify the soil–pile interaction influence under combined static and dynamic loads and to show the effect of the main parameters on the soil–pile behavior. Thus, an elastoplastic material law with a modified Mohr–Coulomb model was chosen for

this research. This study used a 3D model of a pile and embedded in soil. Two different types of piles were used in this study, one was a closed-ended pipe pile that was modeled as a solid volume of a hollow cylinder with a plate at the bottom to close it from the bottom and the second pile was an open-ended one with soil plug. Three construction stages were set for modeling the closed-ended pipe pile: first stage for model self-weight calculation, second stage for the combined static loads, and the third stage for applying the dynamic (earthquake) load. As for the open-ended pipe pile, two solid volumes were proposed to model the soil inside the pipe pile. The first one was for a simulating soil-plug ($4D_{\text{inner}}$), while the second soil column represented the soil cylinder placed on the top of the plugging soil, which was used to perform the analysis during the initial state. The latter volume was deactivated when the pile was installed in the sandbox. Then, the pile was modeled by extracting elements from the cylinder soils (plugging soil and the one above it). Consequently, the other steps were similar to the closed-ended model; full details are presented in Al-Jeznawi *et al.* [9,10]. Static vertical and lateral loads were taken as 50% of the pile allowable capacity (32.5 and 3.5 N for the vertical and lateral loads, respectively). These loads were applied to the pile cap as shown in Figure 1. The dynamic load was represented by the ground acceleration of the Kobe earthquake (0.82 g). The seismogram of this earthquake is shown in Figure 2. New elements (ground surface springs) were created to perform the eigenvalue calculations and also to provide elastic boundaries that were used in the numerical modeling for applying the dynamic load. The nodes’ displacement at the bottom of the soil box is ignored, and the soil’s bottom is roughly considered a fixed end. Free-field elements were also created on the model sides with the direction of applying the ground acceleration to minimize the wave reflection.

The boundary conditions were updated during the three construction stages. For the static analysis, the traditional boundary conditions were used. Then, for the last stage, the static boundary conditions were deactivated and the ground surface spring elements with free field elements were activated during the shaking with 0.02 s as a time step. The solution was derived using a modified Newton–Raphson technique, using a damping ratio of 5% for the soil and pile structure as Rayleigh damping. Interface elements between the soil and pile body were considered using the Coulomb friction coefficient for the analysis. The strength reduction factor, which represents the friction between the soil and the pile, was taken as 0.6 and 0.7 with interface elements between the loose and dense sand, respectively, and

¹ D_{inner} is the internal diameter of the pipe pile.

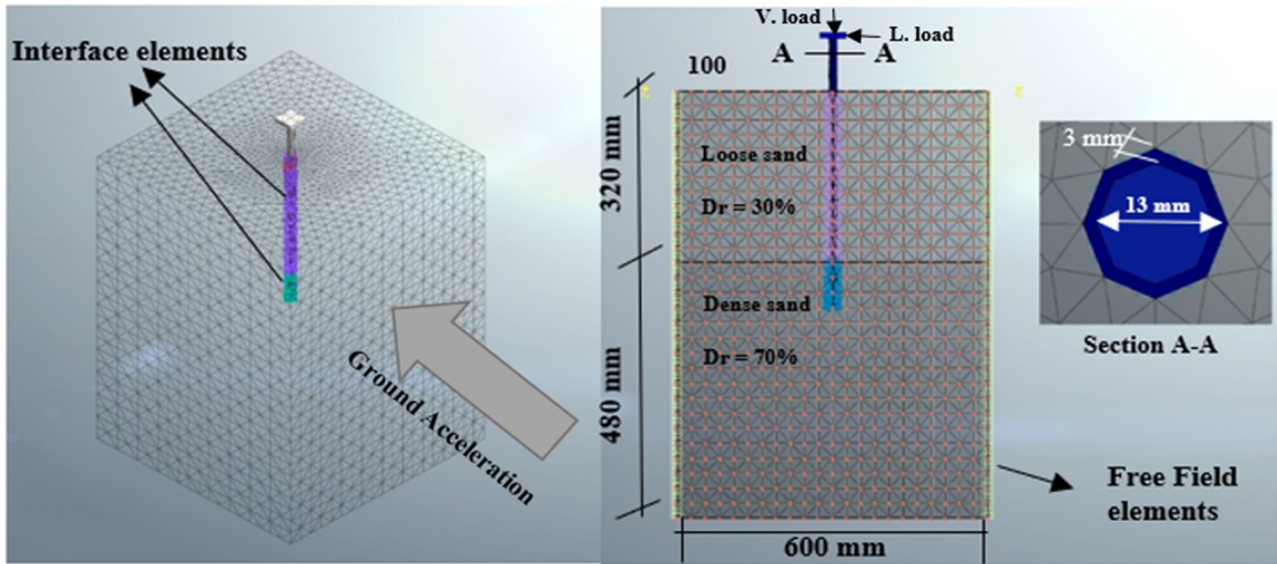


Figure 1: 3D finite element model implemented in the current study.

the pile body (as recommended by the Midas user manual [11]). Figure 1 shows the model’s full configuration.

In the finite element model, a dry sandy soil is used where the top layer is loose sand with a thickness of 320 mm and the bottom is dense sand with a thickness of 480 mm. These layers had relative densities of 30 and 70%, respectively. The driven pile is aluminum, with an outer diameter of 16 mm, an inner diameter of 13 mm, and a length of 500 mm. Since, 100 mm of the pile length was exposed and attached to the pile cap, the length of the embedded pile is 400 mm. The materials and their properties are summarized in Table 1.

validated by comparing it to the experimental findings or site investigation. Hussein and Albusoda [8] performed 1 g shaking table tests in the laboratory to investigate the effect of a soil-closed-end pipe pile system under combined static and dynamic loads. The software results are compared with experimental measurements regarding the acceleration (g), maximum lateral displacement, vertical displacement, and the pile bending moment as shown in Figure 3. Full details related to the bending moment calculations, are described by

3 Results and discussions

3.1 Model validation

In general, before presenting the results of the finite element analysis, the numerical modeling should be

Table 1: Summary of materials used in the current study

Name	Loose sand	Dense sand
Material idealization	Isotropic	Isotropic
Model type	Modified MC	Modified MC
Poisson’s ratio (ν)	0.33	0.33
Unit weight (γ) (kN/m ³)	13.5	16
K_o	0.470	0.426
Drainage parameters	Drained	Drained
Young’s modulus (kPa)	11,000	28,000
Secant elastic modulus in shear hardening (kPa)	5,639	15,037
Tangential stiffness primary oedometer test loading ($E_{oed_{ref}}$) (kPa)	5,639	15,038
Elastic modulus at unloading ($E_{ur_{ref}}$) (kPa)	22,225	59,265
Failure ratio (R_f) (%)	0.9	0.9
Porosity (%)	0.6	0.8
Friction angle (°)	32	35
Dilatancy angle (°)	2	5
Cohesion (c) (kPa)	0.1	0.1

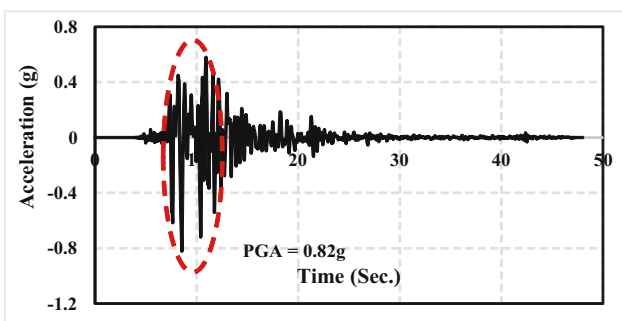
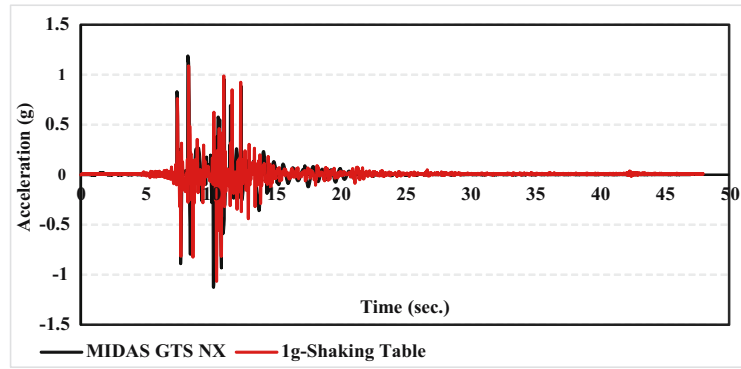
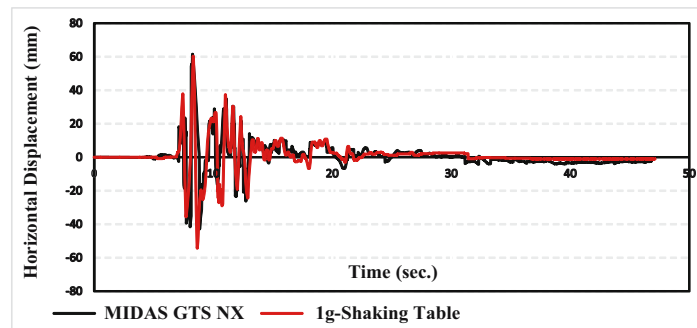


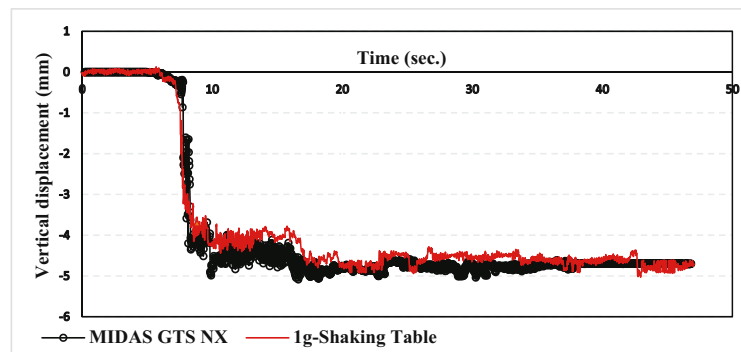
Figure 2: Seismogram of Kobe earthquake history used in the present study [8].



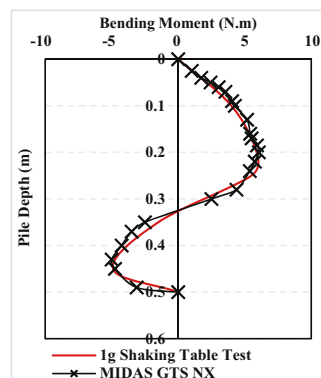
(a)



(b)



(c)



(d)

Figure 3: Model validation: (a) acceleration at the pile head due to Kobe earthquake excitation, (b) maximum lateral displacement at the pile head due to Kobe earthquake excitation, (c) pile settlement due to Kobe earthquake excitation, and (d) bending moment due to Kobe earthquake excitation.

Al-Jeznawi *et al.* [9]. Full details of the 1 g shaking table test are described in [8].

The maximum measured vertical and lateral displacements are 4.23 and 60.3 mm, respectively, and the maximum vertical and lateral displacements obtained from the numerical simulation are 5 and 61 mm, respectively. As for the acceleration (g), the maximum measured value was 1.06 g and the maximum computed value was 1.16 g. Therefore, the provided numerical results showed satisfactory agreement with the experimental findings.

3.2 Shear stress–strain relationship

The complete finite element analysis was performed by first applying static loads to the pile cap and then using the recorded acceleration data from the Kobe earthquake as a horizontal ground acceleration on the bed of the soil box. Figures 4 and 5 present the shear stresses *versus* shear strain, time history of an element on the soil surface

and close to the pile body, and the final state contour lines of the shear stresses within the soil box and plug soil. It is important to note that the soil shear stresses decreased significantly during dynamic excitation until they approached zero. The relationship is in good agreement with the previous studies [12,13]. In Figure 5b, an arching phenomenon was observed; this phenomenon has been described previously by Al-Soudani [14].

The shear resistance developed along the length of the plugged soil (about 508 kPa) is more than the end bearing capacity around the base of the soil plug (414 kPa). Thus, the pile is considered to have failed in a plugged mode.

3.3 Pile frictional resistance

Figure 6a shows the variation of shear stresses in the interface elements with pile length during application of the static and dynamic loads. It is seen that the

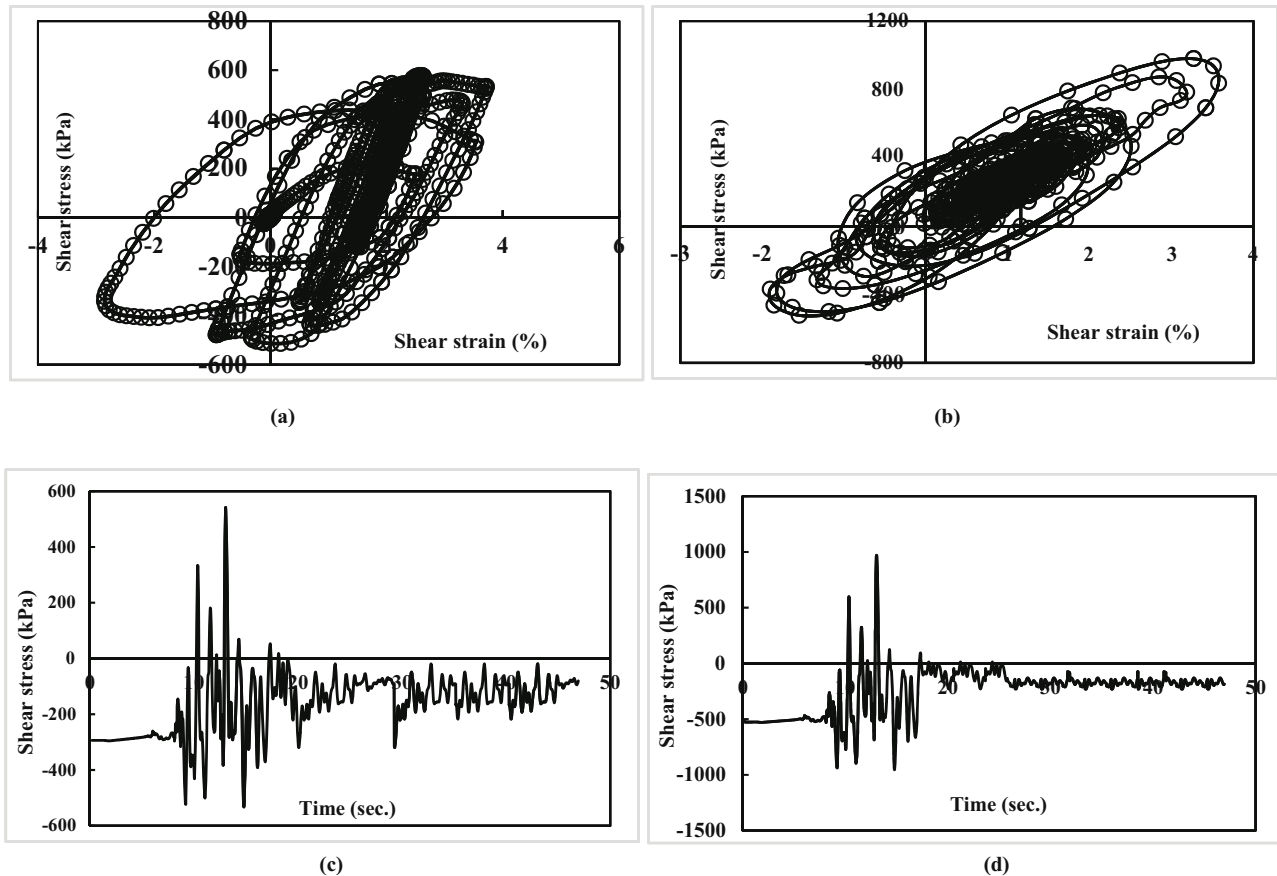


Figure 4: The shear stress–strain relationship with the corresponding shear stress time history: (a) closed-ended pipe pile, (b) open-ended pipe pile, (c) closed-ended pipe pile, and (d) open-ended pipe pile.

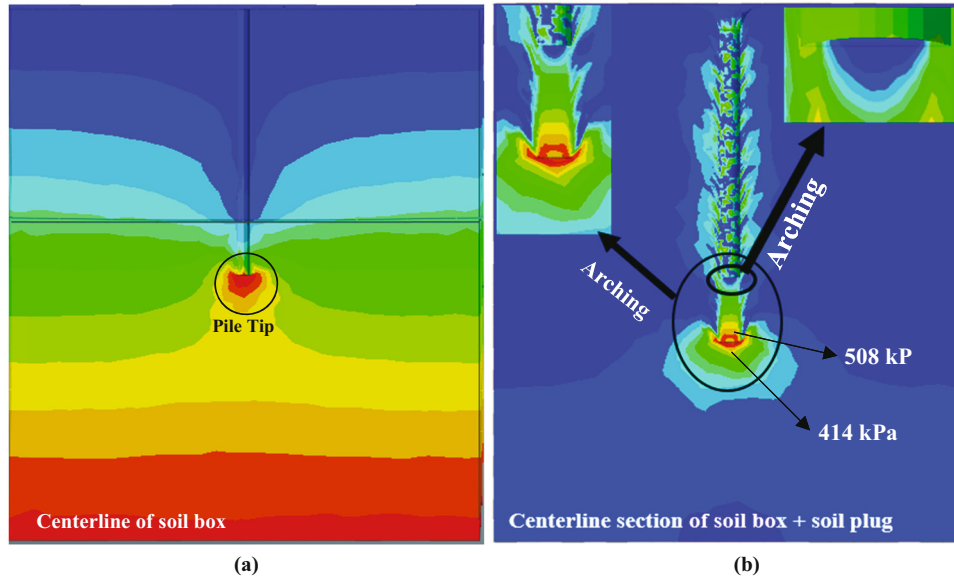


Figure 5: Contour lines of the shear stress in the $y-z$ direction after applying fully coupled static and dynamic loads: (a) closed-ended pipe pile and (b) open-ended pipe pile.

frictional resistance along the soil–pile interface drops drastically during the earthquake and tends to diminish during dynamic excitation until it reaches the minimum values at the final stage. Achmus and Thielen [1] introduced

a 3D finite element model to study the behavior of a single pile in sandy soil and under the effect of axial and vertical loadings. They proposed that simultaneous mobilization of earth pressure, due to the horizontal loading and the skin

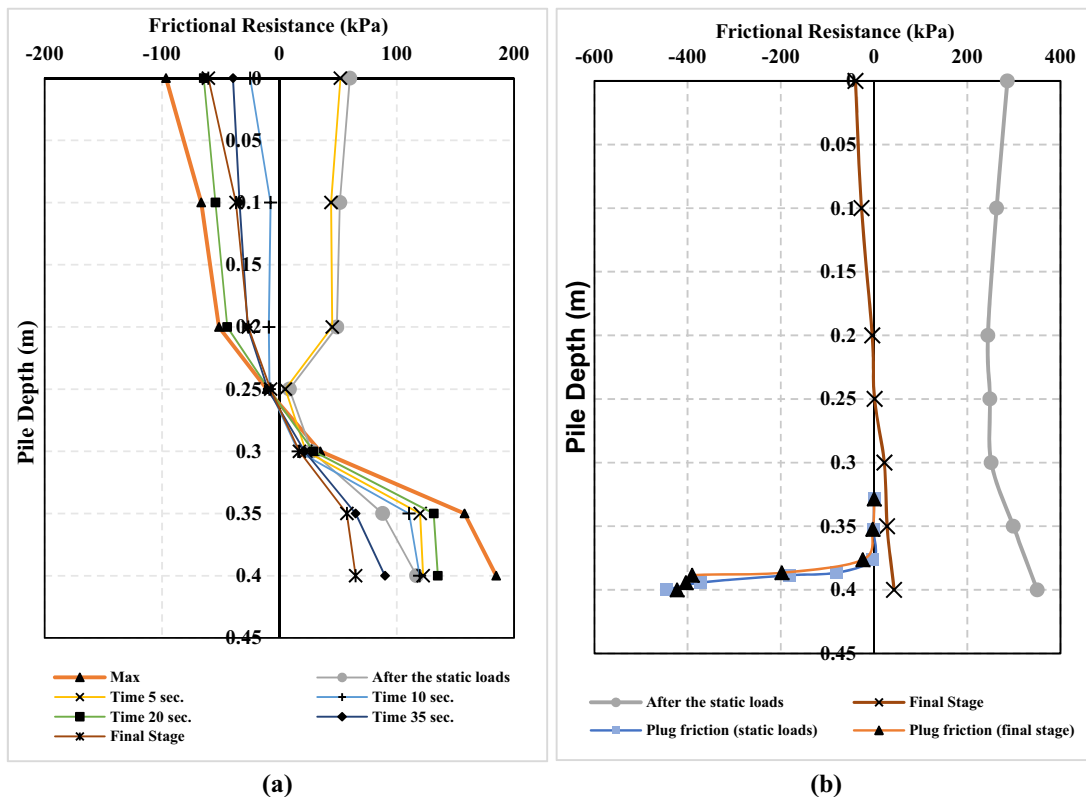


Figure 6: Frictional resistance along the pile length: (a) closed-ended pipe pile and (b) open-ended pipe pile.

friction due to the vertical loading, motivates the interaction effect. Since the loose sand in the top layer has a roughly high initial void ratio (about 0.8) with relative density ($D_r = 30\%$), the particles densified and experienced relative movement concerning the pile body during the earthquake excitation and thus experienced negative frictional resistance to a depth between 0.25 and 0.3 m. This phenomenon occurred with a closed-ended pipe pile after 5 s and during amplification of the ground acceleration. The value increased with the depth through the soil layers and reached the maximum positive value. As for the first 5 s, the behavior of the soil–pile interface was uncertain, which may be attributed to the low values of the static loads which were 50% of the allowable pile capacity in the vertical and horizontal directions as combined with the low applied acceleration during the first 5 s. Therefore, positive skin friction was observed when the ground acceleration increased; these values, reduce until they become negative. Although it is dry sandy soil, it is very important to note that the frictional resistance decreases significantly with dynamic excitation. This may be attributed to the high differential settlement that was observed between the pile and the surrounding soil, which in turn, cause negative friction in the soil layer (loose sand) near the ground surface, while positive frictional resistance was observed at the base layer (dense sand).

Figure 6b shows that the maximum plug resistance in all models is observed at a distance between 0 and 20% of the total plug length. Thus, the high level of load is distributed near the pile tip due to the arching phenomenon and soil densification [15,16]. Although the arching effect inside the soil plug was diminished during dynamic excitation, the plug resistance was maintained higher than the maximum resistance of the surrounding soil. Thus, even with the peak ground acceleration at the time between 8 and 12 s (as shown in Figures 1 and 3a), no further soil was allowed to enter inside the pipe pile. This may be attributed to the simulated high soil particle densification inside the pipe pile, particularly, near the pile tip. It can be concluded that the majority of the pile resistance relaxed was from the outside shaft friction.

4 Conclusion

The findings of an experimental model of a shaking table test were used to develop and validate a finite element model using MIDAS GTS NX software. The simulated response of the pile–soil interaction in the dry situation matched the experimental data quite well. The adopted

model was used to analyze the effect of applying static axial and lateral loads combined with the seismic motion (ground earthquake). Ground surface springs and the free-field elements were considered for dynamic analysis and to minimize the effect of wave reflection. The main conclusions from this study are presented below.

1. Maximum pile settlement was observed between 5 and 10 s during the amplification of the applied ground movement.
2. The pile and soil underwent cycles of compression and tension stresses due to the acceleration amplification. The shear stress–strain path is plotted in Figure 4a. The shear stress–shear strain response is identified by a hysteresis loop; this loop becomes wider and flatter on the x -axis as the shear strain increases.
3. The shear stresses in both models dropped at the end of the dynamic excitation. Due to arching and soil densification of the soil plug, a large level of load is distributed near the pile tip. In the end, dynamic excitation did not affect the plug capacity, and it remained higher than the resistance of the surrounding soil beneath the pile tip.
4. Frictional resistance of the pile was calculated in terms of interface tangential stresses along the pile body. Although the data fluctuated due to the dynamic excitation, a significant drop in the frictional resistance was noticed at the few last time steps.

Funding information: The authors state no funding is involved.

Author contributions: All authors have accepted responsibility for the entire content of this manuscript and approved its submission.

Conflict of interest: The authors state no conflict of interest.

References

- [1] Achmus M, Thieken K. On the behavior of piles in non-cohesive soil under combined horizontal and vertical loading. *Acta Geotech.* 2010;5(3):199–210. doi: 10.1007/s11440-010-0124-1.
- [2] Kokusho T, Iwatate T. Scaled model tests and numerical analyses on nonlinear dynamic response of soft grounds. *Proc Jpn Soc Civ Eng.* 1979;285:57–67. doi: 10.2208/jscej1969.1979.285_57 (in Japanese).
- [3] Kim YS, Roesset JM. Effect of nonlinear soil behavior on inelastic seismic response of a structure. *Int J Geomech.* 2004;4(2):104–14. doi: 10.1061/(ASCE)1532-3641.

- [4] Al-Jeznawi D, Jais IB, Albusoda BS. The slenderness ratio effect on the response of closed-end pipe piles in liquefied and nonliquefied soil layers under coupled static-seismic loading. *J Mech Behav Mater.* 2022;31(1):83–9. doi: 10.1515/jmbm-2022-0009.
- [5] Al-Salakh AM, Albusoda BS. Experimental and theoretical determination of settlement of shallow footing on liquefiable soil. *J Eng.* 2020;26(9):155–64.
- [6] Almashhadany OY, Albusoda BS. Effect of allowable vertical load% and length/diameter ratio (L/D) on behavior of pile group subjected to torsion. *J Eng.* 2014;20(12):13.
- [7] AL-Ghanim AR, Shafiqu QSM, Ibraheem AT. Finite element analysis of the geogrid-pile foundation system under earthquake loading. *Al-Nahrain J Eng Sci NJES.* 2019;22(3):202–7.
- [8] Hussein RS, Albusoda BS. Experimental and numerical analysis of laterally loaded pile subjected to earthquake loading. *Modern applications of geotechnical engineering and construction.* Singapore: Springer; 2021. p. 291–303. doi: 10.1007/978-981-15-9399-4_25.
- [9] Al-Jeznawi D, Jais IB, Albusoda BS. A soil–pile response under coupled static dynamic loadings in terms of kinematic interaction. *J Civ Environ Eng.* 2022;18(1):96–103. doi: 10.2478/cee-2022-0010.
- [10] Al-Jeznawi D, Jais IB, Albusoda BS. The effect of model scale, acceleration history, and soil condition on closed-ended pipe pile response under coupled static–dynamic loads. *Int J Appl Sci Eng.* 2022;19:2022018. [https://doi.org/10.6703/IJASE.202206_19\(2\).007](https://doi.org/10.6703/IJASE.202206_19(2).007).
- [11] Rabii S, Louis AW, Bernhard EB, Bruce AW. *MIDAS User Manual, Version 3.1.* United States: Stanford University; 1997.
- [12] Thilakasiri HS. Kinematic and inertial effects of earthquakes on rock socketed single piles in a two-layered medium. *J Inst Eng (Sri Lanka).* 2010;43(3):3. doi: 10.4038/engineer.v43i3.6968.
- [13] lai S. Similitude for shaking table tests on soil–structure–fluid model in 1g gravitational field. *Soils Found.* 1989;29(1):105–18. doi: 10.3208/sandf1972.29.105.
- [14] Al-Soudani WH. Evaluation the performance of new techniques for open-ended pipe piles in dry sandy soil [dissertation]. Baghdad: Baghdad University; 2020.
- [15] Paikowsky SG, Whitman RV. The effect of plugging on pile performance and design. *Can Geotech J.* 1990;24(7):429–40. doi: 10.1139/t90-059.
- [16] Al-Soudani WH, Albusoda BS. An experimental study on bearing capacity of steel open ended pipe pile with exterior wings under compression load. *Geotech Geol Eng J.* 2020;39:1299–318.